# FORMATION OF TITANIA NANOPARTICLES VIA COMBUSTION THE PYROTECHNIC MIXTURE

V.V. Karasev, A.A. Onischuk, O.G. Glotov, A.M. Baklanov,
E.A. Pilyugina, A.B. Kiskin, V.E. Zarko
Institute of Chemical Kinetics and Combustion,
Russian Academy of Sciences, Novosibirsk 630090, Russia

**Key words:** titania, nanoparticle, aggregate, fractal dimension, electric charge.

## Introduction

Fast development of world industry creates the problems related to the protection of population against consequences of technogenic catastrophes periodically occurring in chemical plants, on transport, etc. The quick response in such emergency cases can be performed on the basis of equipment capable of high operational readiness and production yield. One of the perspective ways to neutralize the dangerous compounds in the atmosphere can be dispersion of sufficient amount of highly active catalytic particles in the air. It is well known that $TiO_2$ nanoparticles in the *anatase* crystal modification exhibit excellent photo-catalytic properties that ensures the ability to destruct harmful substances. The mentioned ability is widely used in air conditioners with photo-catalytic filters of $TiO_2$ (DAIKIN), in self-cleaning $TiO_2$ containing covers for glass, plastic, metal (LG Elite), etc. In the course of photo-catalysis triggered by sun light or UV-lamp radiation ($\lambda < 385$ nm) the various organic substances are oxidized, the viruses and bacteria are destroyed. It is well known that the catalytic effectiveness of the $TiO_2$ powder depends on the particle size. In particular, the commercial $TiO_2$ powder Degussa P-25 contains particles of 25-35 nm size (70-80% anatase; 30-20% rutile); the most effective $TiO_2$ powder Hombikat UV-100 contains particles of 5-10 nm size (100% anatase). At the same time, the well-known fact is the formation of nanosized metal oxide particles in the flame of suspended in air metal powder [1] or in combustion of solid propellants [2]. As a convenient and express way for production of such

kind aerosol particles the firing of the pyrotechnic charges containing pure metal can be considered.

The goal of the present work was to investigate formation of titania nanoparticles in combustion of Ti droplets in the air. The burning droplets were generated via combustion of a metalized pyrotechnic mixture.

**Experimental**

$TiO_2$ aerosol was formed by burning small samples of pyrotechnic mixture in a 20 litres reaction vessel at atmospheric pressure. The reaction vessel was filled before the experiment by filtered air (Figure 1).

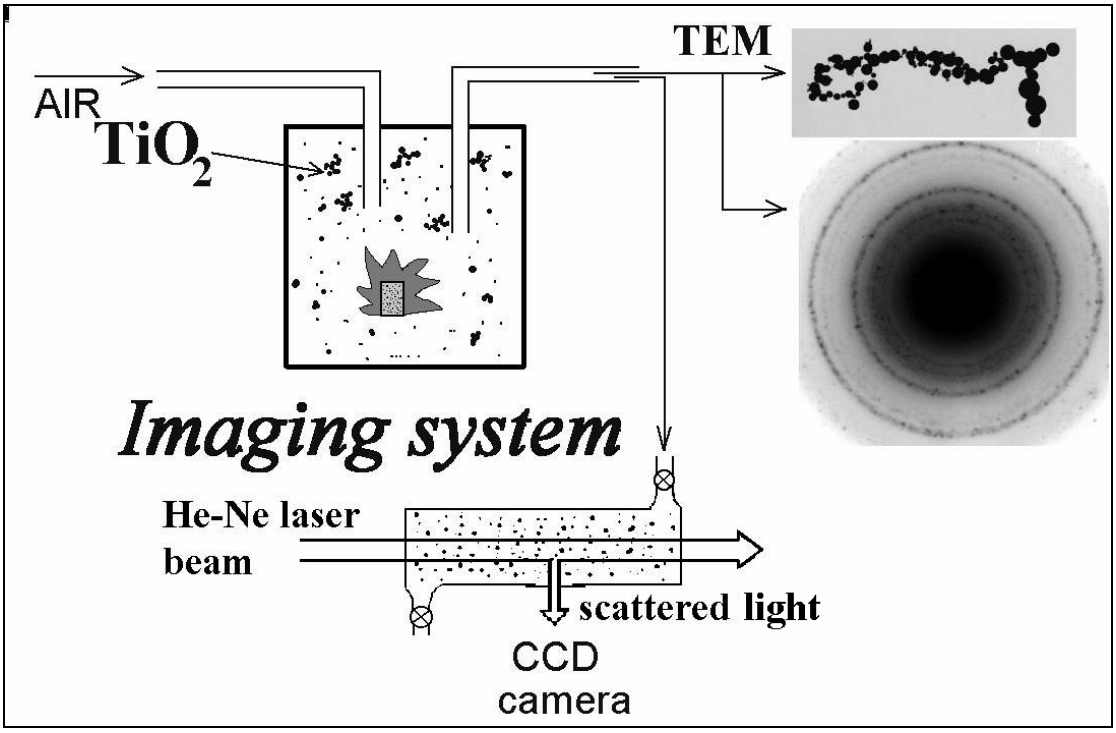


**Figure 1:** Scheme of the experimental set-up.

For filtering, the high efficiency Petryanov aerosol filter [3] was used. The samples to burn (of mass about 0.5 g) contained titanium particles with size of 30 -150 μm. The mass of titanium in a sample was about 75 mg. The sample combustion time was about a few seconds. The combustion of sample was accompanied by ejection of burning Ti droplets of < 200 μm diameter. These droplets moved downwards in the ambient air and generated $TiO_2$ aerosol. The $TiO_2$ aerosol was left in the vessel for certain time (from 0.2 to 20 min after

finishing combustion). Then the aerosol particles were sucked from the chamber and sampled for the Transmission Electron Microscopy (TEM) analysis and for the analysis by video microscope. Sampling for TEM was carried out thermophoretically.

The original video microscopy facility [4, 5] was used to observe coagulation of titania aggregates. In these experiments a probe of aerosol was sucked from the combustion chamber. Then the probe was injected into optically accessible cell designed by Fuchs and Petryanov [6]. In the laboratory set up (Figure 1) a focused He-Ne laser beam passed through the cell volume. A light scattered by aerosol particles at the angle of 90° passed through a flat window to microscope objective and then to CCD camera. The objective drew an image of particles located in the illuminated volume of cell, on the light sensitive CCD-matrix with $15^{\times}$ magnification. The visualization field in the optical cell was $300\times400$ $\mu m^2$ and the focal depth in the object space was about 30 $\mu$m. Spatial resolution of the system was near 3 $\mu$m that allowed obtaining resolved images of aggregates larger than 3 $\mu$m. For smaller size, the aggregates are visible as spots.

The video microscope was used to observe directly the Brownian motion of aggregates as well as their motion in the electric field inside the optical cell. To create the homogeneous electric field two parallel flat electrodes were installed in the cell. The distance between electrodes was 0.25 cm. The mobility equivalent radius was determined from the data on the aggregate Brownian motion. We found that the majority of aggregates are charged. The electric charge of each aggregate was determined by recording the velocity of their movement in the electric field.

## Results

TEM analysis showed that $TiO_2$ is formed as aggregates composed by small primary particles (Figure 2). The size of aggregates was about 0.1-10 $\mu$m, the diameter of primary particles was of 3-30 nm. The specific surface of the aerosol was about 45 $m^2/g$. We determined the aggregate phase composition

from the analysis of electron diffraction images (Figure 3) which was 70% anatase + 30% rutile.

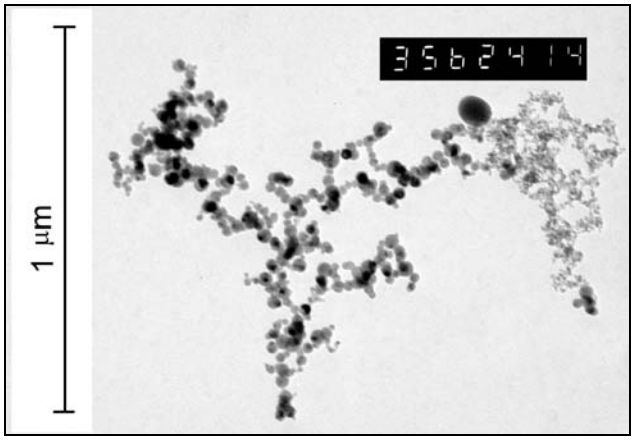


**Figure 2:** TEM image of $TiO_2$ aggregate.

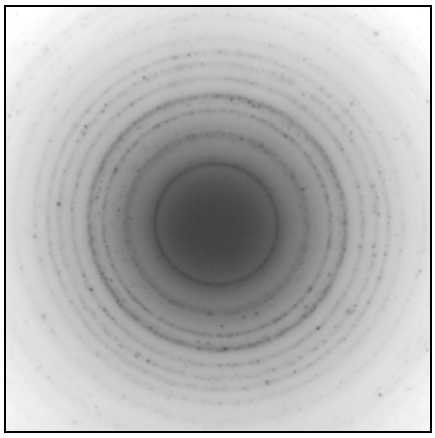

**Figure 3:** Electron diffraction image of $TiO_2$ aggregates composed by anatase (70%) and rutile (30%).

Using the TEM images the effective geometric radius *R* of aggregates was measured as

$$R = \frac{1}{2}\sqrt{LW}\,, \qquad (1)$$

where *L* is the maximum length of the aggregate and *W* is the maximum size of the aggregate perpendicular to *L*. The typical size distribution of $TiO_2$ aggregates is shown in Figure 4.

The aggregate morphology has been described in terms of fractal-like dimension $D_f$ which can be determined from a power type relationship $M \propto R^{D_f}$ between the mass *M* of each aggregate and its radius *R* derived by TEM analysis. The aggregate mass was determined from TEM images by direct measuring the diameter of all the primary particles constituting the

aggregate and subsequent calculating the total aggregate mass. This approach seems to be reasonable when $D_f < 2$ [7, 8]. The mass of aggregates is plotted in Figure 5 in coordinates $\log_{10}M$ - $\log_{10}R$. The fractal dimension $D_f$ determined from this plot equals 1.55 ± 0.02.

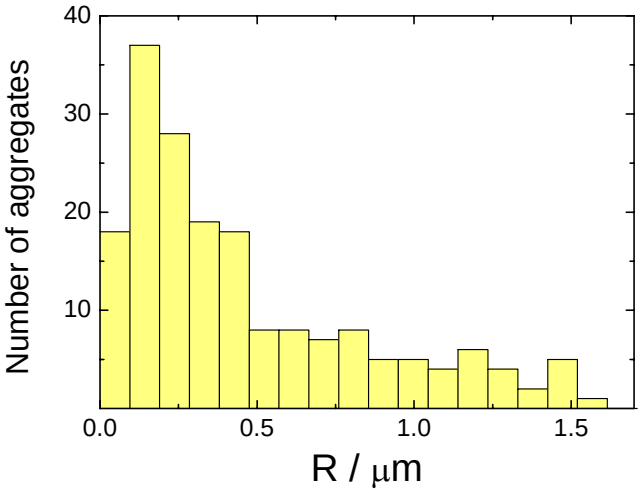


**Figure 4:** Frequency distribution of $TiO_2$ aggregates over geometric radius determined from TEM images. Aggregates were sampled 30 s after the combustion.

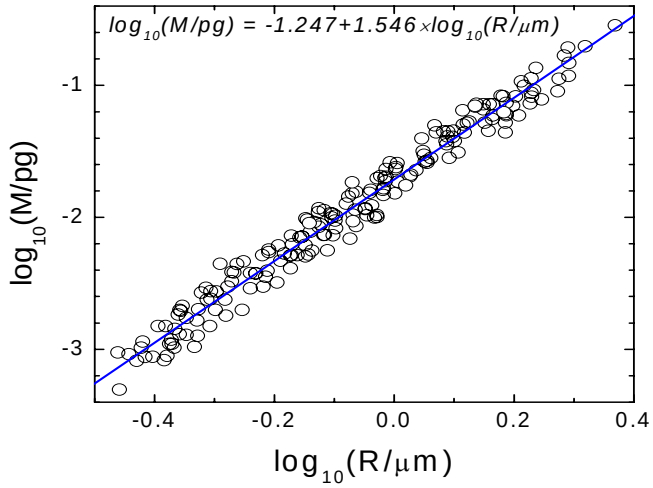


**Figure 5:** Aggregate mass vs. geometric radius

When examining the aggregates, one can determine the average diameter $d_{ag}$ of primary particles for selected aggregate. It was revealed that the $d_{ag}$ value varies from aggregate to aggregate. To demonstrate the difference in $d_{ag}$ for various aggregates, Figure 6 presents frequency distributions of primary particle diameters for two different aggregates. It is seen the essential difference between these two functions. In particular, the mean arithmetic diameter differs twice for the two aggregates (see the caption to Figure 6). The reason for the difference in the average diameter of primary particles in different aggregates is that there exist different groups of primary

particles in aggregates. The size of primary particles in one group is about the same, but it differs essentially from group to group. Figure 2 demonstrates such groups of primary particles in the aggregate. We call these groups as "primary clusters". One may suppose that the primary clusters were originated in the combustion of different titanium droplets and later they formed the final aggregate due to coagulation.

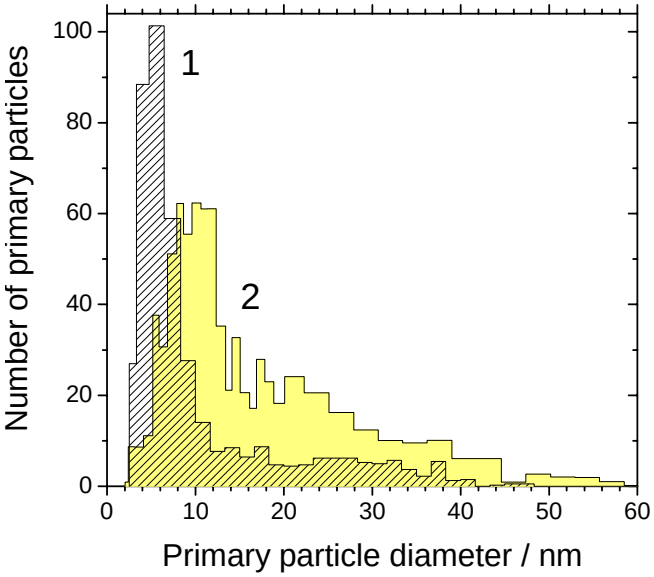


**Figure 6:** Frequency distributions of primary particle diameters for two different aggregates. Histogram 1: mean diameter = 10.3 nm; histogram 2: mean diameter = 19.3 nm.

The mobility equivalent radius of aggregates was determined from the observation of their Brownian motion using the video microscopy. The aggregate diffusion coefficient *D* was determined from the Einstein equation:

$$\overline{(\Delta x)^2} = 2Dt \qquad (2)$$

$\overline{(\Delta x)^2} = \frac{\Delta x_1^2 + \Delta x_2^2 + ... + \Delta x_N^2}{N}$; where $\Delta x_1, \Delta x_2, ..., \Delta x_N$ are successive displacements of the aggregate along horizontal x-axis over time interval *t.* Then the mobility equivalent radius $R_m$ was derived from the expression for diffusion coefficient [8]:

$$D = \frac{kT(1 + \frac{\lambda A}{R_m})}{6\pi R_m \eta} \qquad (3)$$

where $\eta$ is the viscosity coefficient for air, $R_m$ is the mobility equivalent radius, $\lambda$ is the gas mean free path, *A* is the Cunningham correction factor (*A* = 1.257).

In our measurements the time interval was chosen as $t$ = 0.2 s; the number of readings was $N \geq 25$. In this case the video data processing resulted in the error of $R_m$ less than 25%.

Figure 7 shows dependence of mean mobility diameter of aggregates on coagulation time.

Using the video microscope it was possible to observe both the gravity sedimentation and Brownian motion for the same aggregate. Figure 8 shows the gravitational settling velocity *vs*. mobility equivalent radius $R_m$ in the range $0.1 < D_m < 0.5$ μm. By comparing the settling velocity and data presented in Figure 5 we found relationship between geometric radius $R$ and mobility radius $R_m$, see Figure 9. The projection radius $R_s$ (i.e. the radius of equivalent sphere with the same projection area) is also presented in Figure 9 for comparison.

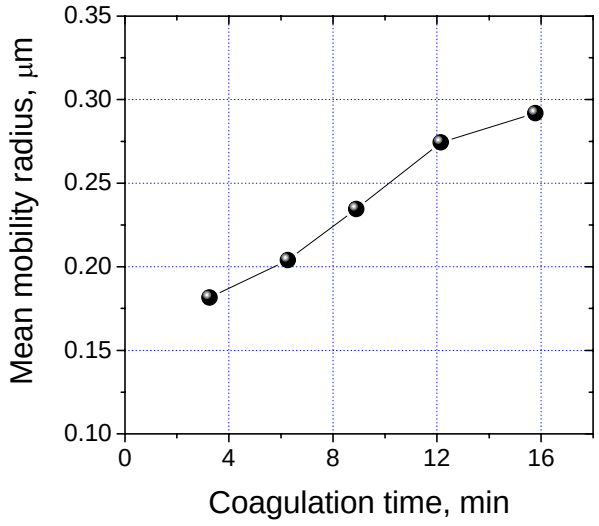


**Figure 7:** Mean mobility equivalent diameter *vs*. coagulation time.

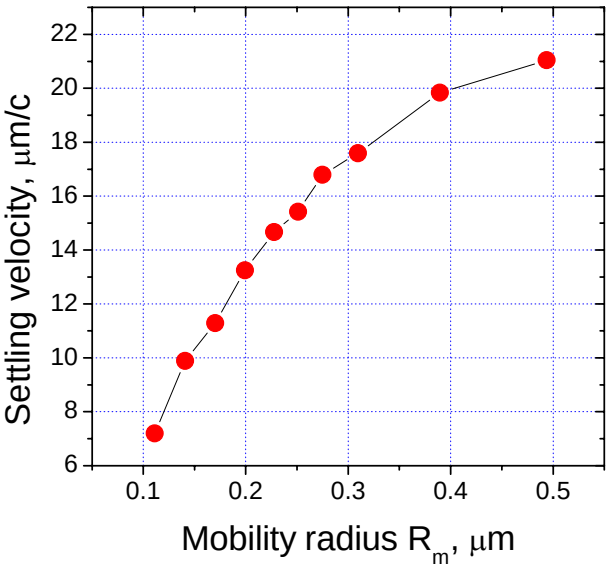


**Figure 8:** Aggregate gravitational settling velocity vs. equivalent mobility diameter $D_m$

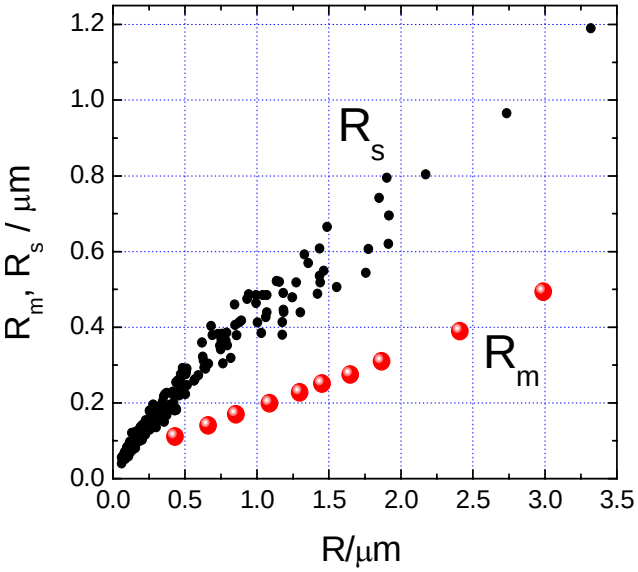


**Figure 9:** Aggregate mobility $R_m$ and equivalent projection $R_s$ radii vs. geometric radius R

Movement of alumina aggregates in homogeneous electric field with intensity of 200 V/cm has been studied by using the video microscope. The aggregate net charge was estimated from the balance between the Coulomb force and the drag force $F_D$:

$$n_{ch}eE = F_D \qquad (4)$$

where $n_{ch}$ is the number of the elementary charges in the aggregate, $e$ is the elementary charge ($4.8\times10^{-10}$ units of CGSE), and $E$ is the electric field intensity. The drag force is [9]:

$$F_D = \frac{6\pi v \eta R_m}{(1+\frac{\lambda A}{R_m})} \qquad (5)$$

where $v$ is the aggregate velocity, other parameters see in (3).

The results of charge measurements are presented in Figure 10 in coordinates aggregate charge $n_{ch}$ - aggregate radius $R_m$.

**Discussion**

It was found in this study that the fractal-like (or Hausdorf) dimension of titania aggregates is $D_f \approx 1.55$ (Figure 5). In general, the value of $D_f$ depends on the mechanism of aggregate formation. The mechanism of diffusion-limited cluster-cluster aggregation (DLCCA) results in $D_f \approx 1.8$ [6]. The DLCCA mechanism assumes that the aggregates approach each other due to the

Brownian diffusion and there are no long-range interactions between colliding aggregates. On the other hand [10 - 12], long-range attractive interaction between coagulating particles or aggregates results in a smaller value of fractal-like dimension. Thus, we can explain the experimentally determined relatively low fractal dimension by the Coulomb interactions between colliding aggregates.

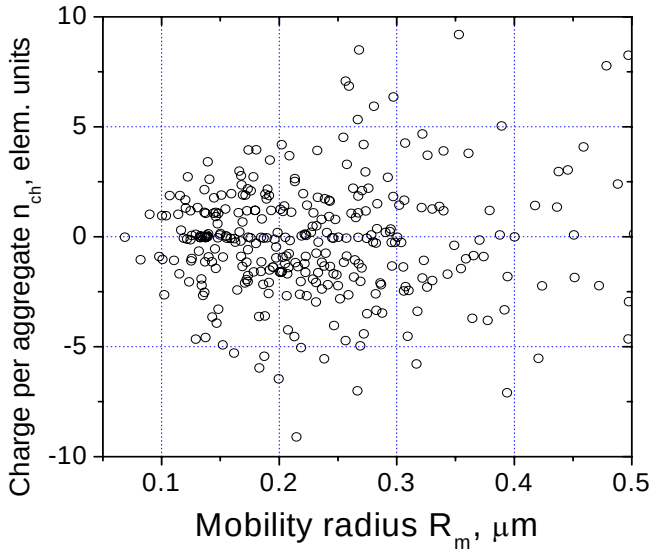


**Figure 10:** Scattering plot in coordinates aggregate charge $n_{ch}$ - equivalent mobility radius $R_m$.

Aerosol particles in bipolar ion atmosphere are to come to steady-state condition. For particles with size larger than 0.05 μm the distribution of charges at the steady-state condition corresponds to the dynamic electrical equilibrium described by the Boltzmann law (see, for example, [8, 13-15]:

$$f(q) = \frac{1}{\Sigma}\exp\left(-\frac{(q)^2}{d_E kT}\right) \tag{6}$$

$$\Sigma = \sum_{-\infty}^{\infty}\exp\left(-\frac{(q)^2}{d_E kT}\right) \tag{7}$$

where *f(q)* is the fraction of particles which have the charge *q*, *k* is Boltzmann constant, *T* is temperature, $d_E$ is the charging equivalent diameter. It was shown [16, 17] that the steady-state charging equivalent diameter for aggregates in bipolar ionic atmosphere is approximately equal to the aggregate mobility diameter.

Figure 10 shows a scattering plot in coordinates aggregate charge $n_{ch}$ - mobility equivalent radius $R_m$. It is possible to select a narrow range of radius in

this charge - radius diagram. In this case we obtain the charge distribution for the selected radius range. Figure 11 demonstrates a charge distribution for aggregates with the mobility radius being taken in the range $0.15 < R_m < 0.20$ μm .

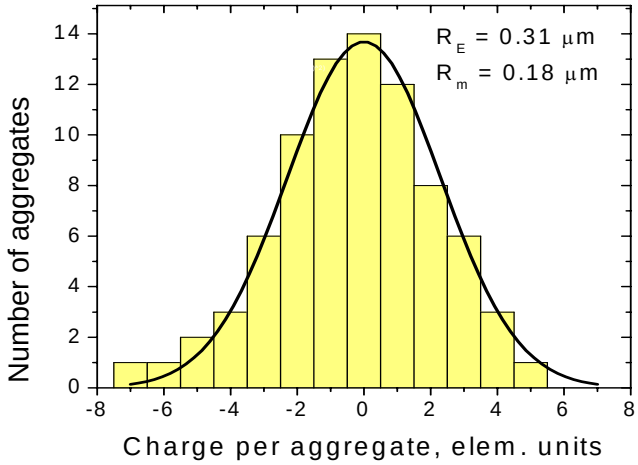


**Figure 11:** Charge distribution for aggregates with the mobility radius being in the range $0.15 < R_m < 0.20$ μm.

This charge distribution can be fitted by the Gaussian function for the room temperature and $R_E$ = 0.31 μm. The charging equivalent radius $R_E$ exceeds the average mobility radius $R_m$ = 0.18 μm. In other words, the charge distribution for these aggregates is wider than equilibrium being intermediate between droplet combustion temperature and room temperature equilibrium. Figure 12 shows $R_E$ versus $R_m$ dependence. Thus, the ratio $R_E/R_m$ =1.65 for the investigated range of the aggregate radii $0.1 < R_m < 0.3$ μm.

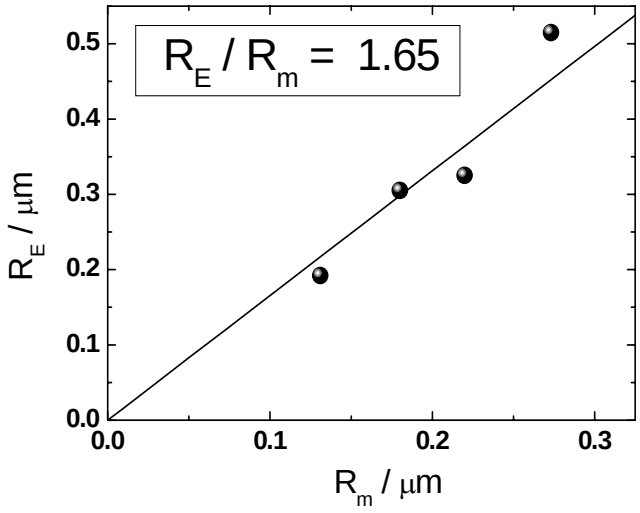


**Figure 12:** Aggregate charging equivalent radius vs. mobility equivalent radius.

The reason for the above-equilibrium charge spectrum formation is believed to be as follows. The reaction zone around the burning metal droplet is

characterized by the high ion concentration. When increasing distance from the reaction zone both temperature and ion concentration drops down. Therefore, aggregate charge distribution becomes wider than the equilibrium distribution for this decreased temperature.

## Conclusions

By means of the video observation charge distributions of $TiO_2$ aggregates synthesized by Ti based pyrotechnic mixture combustion have been determined. The charge distribution of titania aggregates is above equilibrium being wider than room temperature equilibrium 1.65 times.

From the video observations and TEM data the aggregate mobility $R_m$ equivalent projection $R_s$ geometric R radii were determined for the aggregates under study. It was determined that the ratio between these radii
is about $R : R_s : R_m = 6:2:1$.

## References


1. Zolotko A. N., Vovchuk Ya. I., Poletaev N. I., Florko A. V., Altman I. S. “Synthesis of nanooxides in two-phase laminar flames”. *Combustion, Explosion and Shock Waves*, 1996, Vol. 32, No 3.
2. Karasev V. V., Onischuk A. A., Glotov O. G., Baklanov A. M., Zarko V. E., Panfilov V. N., “Charges and fractal properties of nanoparticles - combustion products of aluminum agglomerates”. *Combustion, Explosion and Shock Waves*, 2001, Vol. 37, No. 6, 734-736.
3. Kirsch, A. A., Stechkina, I. B. and Fuchs, N. A. "Efficiency of aerosol filters made of ultrafine polydisperse fibres". *J. Aerosol Sci*. 1975, **5**, P.119 - 124.
4. Onischuk A. A., Strunin V. P., Karasev V. V., Panfilov V. N. "Formation of electrical dipoles during agglomeration of uncharged particles of hydrogenated silicon". *J. Aerosol Sci.,* 2001, **32,** 87 - 105.
5. Onischuk A. A., S. di Stasio, Karasev V. V., Baklanov A. M., Makhov G. A., Vlasenko A. L., Sadykova A. R., Shipovalov A. V., Panfilov V. N. "Evolution of structure and charge of soot aggregates during and after formation in a propane/air diffusion flame". *J. Aerosol Sci.,* 2003, **34,** 383 - 403.

6. Friedlander S. K. *Smoke, dust, and haze*. New York - Oxford, Oxford University Press, 2000.
7. Rogak S. N., Baltensperger U. and Flagan R. C. "Measurement of mass transfer to agglomerate aerosols". *Aerosol science and technology* 1991, **14,** 447 - 458.
8. Fuchs N. A. *The mechanics of aerosols*; Pergamon Press: Oxford, 1964.
9. Reist, P. C. Aerosol Science and Technology, McGraw-Hill, Inc. 1993.
10. Hurd A. J. and Flower W. L. "In Situ Growth and Structure of Fractal Silica Aggregates in a Flame". *Journal of Colloid and Interface Science,* 1988, **122,** 178 - 192.
11. Zhang H. X., Sorensen C. M., Ramer E. R., Olivier B. J. and Merklin J. F. "In situ optical structure factor measurements of an aggregating soot aerosol". *Langmuir,* 1988, **4,** 867 - 871.
12. Julien R. and Meakin P. "Simple models for the restructuring of three-dimensional ballistic aggregates". Journal of Colloid and Interface science 1989, **127**, 265 - 272.
13. Hussin, A., Scheibel, H. G., Becker, K. H. and Porstendorfer, J. "Bipolar diffusion charging of aerosol particles - I: Experimental results within the diameter range 4 - 30 nm". *J. Aerosol Sci.,* 1983, **14,** 671 - 677.
14. Liu, B. Y. H. and Pui, D. Y. H. "Electrical neutralization of aerosols". *J. Aerosol Sci.,* 1974,**5,** 465 - 472.
15. Wen, H. Y., Reischl, G. P. and Kasper, G. "Bipolar diffusion charging of fibrous aerosol particles - I. Charging theory". *J. Aerosol. Sci.,* 1984, **15,** 89 - 101.
16. Wen, H. Y., Reischl, G. P. and Kasper, G. "Bipolar diffusion charging of fibrous aerosol particles - II. Charge and electrical mobility measurements on linear chain aggregates". *J. Aerosol. Sci.,* 1984, **15,** 103 - 122.
17. Rogak, S. N. and Flagan, R. C. "Bipolar diffusion charging of spheres and agglomerate aerosol particle". *J. Aerosol Sci.,* 1992, **23,** 693 - 710.